LBL-15283

Conf-821161--2

Lawrence Berkeley Laboratory

UNIVERSITY OF CALIFORNIA

LBL- 15283

DE83 005861

Presented at the Conference on High-Energy Physics with Nuclear Emulsion, Cairo, Egypt, November 11-29, 1982

SPECTATOR-VELOCITY PIONS FROM HEAVY IONS

John Rasmussen, James Ridout, Don Murphy, and Hafez M.A. Radi

November 1982

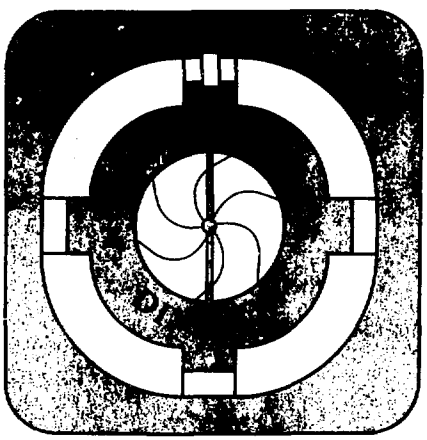

Prepared for the U.S. Department of Energy under Contract DE-AC03-76SF00098

LBL-15283

Spectator-Velocity Pions from Heavy Ions

John Rasmussen, James Ridout, and Don Murphy

Nuclear Science Division
Lawrence Berkeley Laboratory
University of California
Berkeley, California 94702

and

Hafez M.A. Radi

Kuwait University, Kuwait

This work was supported by the Director, Office of Energy Research, Division of Nuclear Physics of the Office of High Energy and Nuclear Physics of the U.S. Department of Energy under Contract DE-AC03-76SF00098.

SPECTATOR-VELOCITY PIONS FROM HEAVY IONS

John Rasmussen, James Ridout, and Don Murphy

University of California Lawrence Berkeley Lab

Berkeley, CA 94720, U.S.A.

and

Hafez M. A. Radi

Kuwait University, Kuwait

1. Introduction

I am most grateful for the invitation to come to Egypt to participate in this conference on high energy physics research and to have the opportunity of telling you about some of our research. For the past five years my close associates and I at the Berkeley BEVALAC have been pursuing various studies of pion production by heavy ions.[1-6] Today I wish to focus my remarks on pions in the velocity regions of target and projectile, where strong spectral features appear.

Our main studies have been in the projectile-velocity and center-of-mass regions, measuring pions near 0^{o} in a magnetic spectrometer. We have made only a modest beginning to study pions in the target-velocity region by searching for stopped pions from emulsion interactions of 1.8A GeV Fe ions. In this latter work we are indebted to Dr. Harry Heckman for invaluable assistance in generously making available his emulsions and micro-

scopes and in directing his scanners in the anomalon studies to flag apparent slow pions, so that undergraduate research student James Ridout could further study the slow pions by tracing them to their stopping and to a possible star. Fig. 1 shows a photomicrograph of a stopped-pi^- event initiated by an ^{40}Ar beam from earlier work of Heckman and colleagues. Seeing this picture on the wall by Heckman's office had much to do with inspiring us to look for more such events.

From early on it became clear that we were dealing with a Coulomb effect of spectator fragments. In some of the earliest, and now classic, studies[7,8] on the BEVALAC Drs. Harry Heckman, Douglas Greiner, Peter Lindstrom, and their collaborators showed that Gev-energy heavy ions often fragmented, with the spectator pieces continuing on within a narrow forward cone with velocities in a narrow distribution about the projectile velocity.[7,8] Thus, our observation of a prominent pi^- peak near beam velocity and a pi^+ depression in the cross section there evidently was a result of Coulomb forces from the projectile spectator fragments. We shall discuss the theory in more detail in a later section.

2. Stopped-pion Studies

The target counterpart of the beam-velocity pions we studied are pions of one to a few MeV in the laboratory. At these low energies there is a good chance that the pions will stop in the emulsion stack. After stopping, the pi^+ undergoes decay to a muon, which in turn decays to a positron. This succession of decays leaves a very characteristic identification. After stopping, the pi^- will cascade down through Bohr orbits of an atom of the stopping medium and from a low orbit will undergo a nuclear disintegration in which usually one or more energetic particles emerge to form a "star." Of course, some of the time the pion's rest mass of 140 MeV can be carried off by neutrons and gamma rays and be missed in emulsions. Scanners can often recognize the characteristic multiple-scattering or meandering nature of a slow-pion track. This meandering makes the problem of energy determination a little greater, since one must try to estimate the track length of a wandering track.

Stopped pion emulsion studies with cosmic rays were published long ago by Friedlander and his collaborators.[9] One aspect they found remarkable was the presence of pi^+ at sub-barrier energies in numbers greater than would be expected for simple quantum mechanical tunneling. More exten-

sive work has been reported by Kostanashvili and others.[10-12] She has presented work for emulsions irradiated with protons at 660 MeV and 9 GeV and with pi^- at 60 GeV.

Our work suffers from quite low statistics and is presented here to stimulate others to take up the challenge of stopped pion work with heavy ions. As mentioned above, we worked in conjunction with Dr. Heckman's anomalon scanning program. The projectiles were ^{56}Fe ions of kinetic energy 1.8A GeV incident upon Ilford G5 emulsion stacks of pellicles either 25 cm x 7 cm x 600 microns or 12 cm x 7 cm x 600 microns. In all we examined 105 pions. Of these, only 15 proved acceptable in that they originated in an Fe-produced star and they stopped in the emulsion with a recognizable signature. This total is made up of 9 pi^- and 6 pi^+.

2.1 Range Measurement and Energy Determination

The distance that a stopped pion has traveled from its formation serves to determine its initial energy. The ranges of the 15 acceptable pions were measured using a microscope reticule calibrated with a stage micrometer. Distances along the meandering tracks were measured by dividing the track into a number of nearly straight segments. In calculating the distances

the shrinkage was accounted for by multiplying all vertical distances by a shrinkage factor equal to 600 microns divided by the measured pellicle thickness. The energy of the Fe projectile at the interaction point was measured for each event by determining the distance the Fe travelled in emulsion before interacting.

2.2 Angle Measurements

Pion emission angle measurements were made using a goniometer attached to the microscope. Both the angle from the beam direction projected onto the horizontal plane, θ , and the corresponding polar angle, α , were obtained for each event.

2.3 Estimation of the Effective Charge

For each pion accepted, the Fe "star" from which it emerged was examined in order to decide whether a heavy emulsion nucleus (Br or Ag) was involved. Ten of the 15 events were determined to involve heavy targets due to the presence of more than eight target-associated fragments ($N_h > 8$). The remaining five events may involve either heavy or light target (HCNO) collisions.

For each of the heavy-target events we attempted to estimate the residual target charge, Z_{eff}, by determining the total charge that emerged from each collision and subtracting this value

from the sum of the atomic number of Fe and the average of the atomic numbers of Br and Ag.

Estimating the charge that emerged from a collision involved first determining the total multiplicity of the event. Thus, all tracks emerging from each "star" of at least 6.7 microns in length were counted. The minimum resolvable track length is less than this value outside of extreme forward angles for horizontal tracks, but increases with the angle of dip.

It then remained to obtain an estimate of the charge represented by each of the counted multiplicities. This charge could not be determined exactly, since for all tracks outside of about 6°, hence not necessarily near beam velocity, there is considerable difficulty with making charge determinations, especially for those tracks that cannot be traced to the end of their range. There is also the problem of the presence of negative pions and the corresponding created positive charge that must be taken into account. For the purpose of estimating the multiplicity of alpha particles and higher charged fragments, cosmic-ray results for projectiles of $Z > 19$, given by Powell et al.[13] were chosen. From these data, we took the doubly charged fragments to comprise about 8% of the tracks. We neglected correcting for the expected small fraction of Li, Be, etc. To correct for the

fast pions, which are indistinguishable from other fast tracks, we took the results of streamer chamber studies with heavy ions at E/A of 1.8 GeV that about 10% of total tracks are negative pions.[14]

We summarize then the expressions used to determine the Z_{eff}:

$$Z_{OUT} = N - 0.2N + 0.08N + Z_{frag} - 1,$$

where N is the multiplicity, the second term is the correction for pions, the third term is the correction for the alpha particles, and Z_{frag} is the charge of the major projectile fragment. Then the charge of the target residue was estimated as follows:

$$Z_{eff} = (Z_{Br} + Z_{Ag})/2 + Z_{Fe} - Z_{OUT}$$

2.4 Results

Our pion energy distributions are shown in Figs. 2 and 3, along with the Kostanashvili et al.[12] data. Fig. 2 refers to heavy-target events and Fig. 3 to undetermined-target events.

In Figs. 4 and 5 the angles of pi^+ and pi^-, respectively, are shown, with the a) part for pions with less than 11.6 MeV of energy and the b) part for pions with energies between 10 MeV and 21.7 MeV. The upper lines plot the projected angle θ, and the lower line the polar angle α.

It is difficult to draw conclusions from our

few events. It does seem that we have less suppression of pi^+ relative to pi^-. This is qualitatively understandable, since the initiating proton and pion projectiles of the Georgian work would not be as likely to disintegrate Ag and Br to the extent that Fe ions would. For central collisions, where there is but little residual target charge, the ratio of the two charged pions could approach unity, though one would expect some excess of negative pions, since the neutron-to-proton ratios of projectile and targets exceed one.

Little can be said about angular distributions, but there is an indication in Fig. 5a that the lower-energy pi^- are somewhat forward-peaked, in contrast to the Georgian work, with its slight backward peaking. The expectation from our spectrometer studies on convoy pions near the projectile velocity would be that the stopped pi^- would be slightly forward peaked, corresponding to a small forward momentum imparted to the target residue by the heavy ion projectile. The single hadron projectiles of the Georgian work would not impart significant forward momentum to the residues, and their backward peaking could be due to absorption shadowing effects.

In Fig. 6 we present the results of the estimates of the charges of target residues. Each

pion event we accepted is shown, with its abscissa the residue charge and its ordinate the pion energy. In parentheses by the data points is given the polar angle of emission with respect to the beam direction. The letter relates to the azimuthal correlation with the emission of evaporated particles from the target. The letter H denotes that the pion was emitted in the azimuthal quadrant with the highest multiplicity of evaporation tracks; the letter L, the lowest; and the letter A, one of the two adjacent quadrants. Only one pi^+ is actually "sub-barrier", namely, the lowest dot at Z_{eff} of 9. It may be that the residual charge is really lower due to uncertainties in our estimates. Again the statistics are clearly insufficient for many conclusions, but there does seem to be a tendencey for the pi^- to be the most abundant for residual charges greater than 20, and the energies of the pi^- are lower than the lone pi^+ in this region.

I would certainly encourage the Cairo group to pursue stopped-pion studies, perhaps with the carbon ion exposures from Dubna, the highest energy heavy ions yet available. I hope I have showed that the heavy ions give features quite distinct from the single hadron exposures studied in refs. 10-12.

3. Convoy Pions in the Projectile Frame

Now I should like to recount one of the exciting chapters of our studies of 0^{o} pion spectra from heavy ions at the BEVALAC. With our principal collaborators, Profs. Benenson, Nolen, and Kashy from Michigan State University and Dr. Koike from the Institute for Nuclear Studies, Tokyo, we set up a few years ago a large 180^{o} magnetic spectrometer with a 3-plane wire chamber in the focal plane and another 3-plane wire chamber some distance behind to establish emission angle. Backing up the wire chambers was an 11-element scintillation range telescope to identify pions by energy-loss and range. Fig. 7 shows a schematic view of the spectrometer, and Fig. 8 shows a photograph of four of our young scientists sitting in front of the spectrometer.

Prior to our 0^{o} studies pion spectra, whether produced from protons or heavy ions, were rather smooth and featureless. We were at first startled by the spectral irregularities of pions near beam velocity. Soon we realized that it was a natural consequence of the Coulomb force from projectile fragments that pi^{-} would be enhanced and pi^{+} would be suppressed near beam velocity.

I show just two sample pi^{-} spectra from refs. 4 and 6. Fig. 9 is an isometric plot with contour

map beneath, and the data are for the Ne + NaF system at lab kinetic energy of E = 138A MeV. The lab rapidity axis runs along the back right edge, and the perpendicular momentum axis runs down along the back left edge, with the scale labeling in front. One sees a single prominent peak appearing at the beam velocity. The remainder of the spectrum falls off smoothly and exponentially toward higher momenta. The ripples are probably statistical fluctuations. Fig. 10 is a similar spectrum taken at the higher beam kinetic energy of 655A MeV. Now the beam velocity peak has moved along the back axis to nearly the maximum pion rapidity we could measure with our old spectrometer. Besides the beam velocity peak we now see additional bumps at lower energy, maximizing at 90° center-of-mass at a perpendicular momentum of about 0.45 in natural units of the pion rest mass times the speed of light. In ref. 6 the mid-rapidity bumps are discussed, but here we shall keep attention on the convoy pions in the projectile rapidity region.

Theoretical papers of Bertsch[15], Libbrecht and Koonin[16], Cugnon and Koonin[17], Gyulassy and Kauffmann[18], and Bawin and Cugnon[19] all have treated these Coulomb effects on pion spectra from heavy ions. All treatments get a qualitatively

satisfactory explanation of the beam-velocity data. However, in many details it is still an open problem for theory to extract the maximum information from the data. For example, in Monte Carlo trajectory studies and associated study of the classical Jacobian in the three-center Coulomb problem Radi, Frankel, Sullivan, Song, and I presented[20] reasons for caution in applying the analytical approximation formulas of ref. 18 under certain conditions. Instead of the known bound projectile fragments, in refs. 17 and 18 the projectile spectators are represented by thermally expanding charge distributions. Thus, in this paper I will mainly discuss the restricted treatment by Radi, Sullivan, Frankel, Hashimoto, and me[21]. This treatment is restricted to the lightest target data (carbon) available with projectiles of ^{20}Ne and ^{40}Ar. That is, we ignore the Coulomb effects of any target remnants and just treat the two-body problem between pion and projectile fragments. We calculate the projectile fragment distributions from a firestreak model computer code that gives good agreement with direct measurements of fragmentation. We assume the fragments to have a Gaussian distribution in velocity about the projectile velocity with the width dependent on fragment mass through the expressions developed by Greiner, Lindstrom,

Heckman, Cork, and Bieser[22].

$$p \propto \exp\left[-\frac{\beta_F^2}{2\alpha_F^2}\right] \qquad (1)$$

$$\alpha_F = \frac{\sigma_0 c}{m_N c^2}\sqrt{\frac{A_0 - A_F}{A_F (A_0 - 1)}} \qquad (2)$$

where $\beta_F = v_F/c$ is the fragment velocity ratio to the speed of light, α_F is the velocity dispersion with A_0 the projectile mass, A_F the fragment mass number, and σ_0 an empirical constant, related to the Fermi momentum by theory.

We then average the Sommerfeld Coulomb parameter over the fragment momentum distribution to get a result in terms of an error function.

$$\langle \eta_\pm \rangle_{\beta_F} = \pm\left[\frac{Z_F e^2}{\hbar c}\right] \frac{\mathrm{erf}\left[\beta_{\pi\pm}/\sqrt{2}\,\alpha_F\right]}{\beta_{\pi\pm}} \qquad (3)$$

Finally, we do a computer average over all products. The expression is somewhat too lengthy to reproduce here, but it is given in full in ref. 21. Fig. 11 shows the fit of the theory to Ne + C data at 280A MeV. It seems that a somewhat smaller value of the parameter σ_0, namely, 60 MeV/c gives better agreement with the data than the value of ref. 7 for the fragments themselves. It must be borne in mind that we are measuring with

the pion spectra something different from the inclusive fragmentation measurements. That is, we are selecting those fragmentations accompanied by pion production, and the pions are sensitive to the primary excited fragment dispersion before subsequent evaporation of protons and neutrons. In a next generation pion study planned now by Hashimoto and colleagues at the HISS (superconducting) spectrometer, pions will be measured in coincidence with identified projectile fragments, so the above theory can be put to a more severe test. I should point out that the formulas and results of refs. 17 and 18 are certainly applicable in the projectile velocity region, but one should reinterpret their mean thermal expansion velocities as proportional to the dispersion of the bound fragment velocities.

As an example of Monte Carlo trajectory studies, I show just a few figures from the most recent work[20] of Radi and collaborators that should appear soon in Phys. Rev. C. This work of ours differs from that of ref. 17 most significantly in that it imposes a strong pion absorption that does not allow trajectories to propagate through nuclear material. Our trajectories were calculated from non-relativistic equations of motion, whereas in ref. 17 relativistic equations were used. However, our study was mainly directed

at pions near rest in the c.m. frame, and we dealt with a lower energy reaction than did ref. 17. That is, our calculations were for the ^{20}Ne + NaF at E = 655A MeV. We were mainly concerned with resolving a discrepancy between experiment[5] and theory[17] regarding the pi^- to pi^+ ratio for pions at rest in the c.m. frame. Theory predicted a ratio of 5.5, and experiment gave 1.5 for ^{40}Ar on ^{40}Ca at E = 1.05A GeV. Indeed our new theoretical calculations did lead to satisfactory agreement with experiment on this ratio, and we attribute this better agreement to the inclusion of strong absorption of pions in nuclear matter, both fireball and spectator.

Our Monte Carlo calculations were not designed for optimum study of the projectile velocity region, since we calculated non-relativistically in the c.m. frame and we did not include projectile-fragment velocity dispersion nor attempt to reproduce experimental fragmentation inclusive cross sections as in our above-mentioned work in ref. 21. Nevertheless, it is interesting to examine our Monte Carlo results in the projectile-velocity region for the qualitative insights they afford. Fig. 12 is a dot plot of Monte Carlo events on a parallel-velocity vs. perpendicular-velocity plane for a particular impact parameter

of 0.4 times grazing value. The lowest inset is for neutral pions, and the initial and final velocities are the same because there is no Coulomb deflection. The density of points increases with increasing perpendicular velocity because of the three-dimensional geometry. The upper left frames are initial velocities for surviving trajectories. Note especially the large region around spectator velocities where pi^- orbits are either pulled in to be absorbed by the spectator or end up orbiting the spectator. The upper right frames show the final distributions, and one clearly sees the Coulomb exclusion of pi^+ near spectator velocities and the bunching of points there for pi^-.

In Fig. 13 these Monte Carlo results for pi^- along the 0^o direction are displayed as a histogram and smooth curve, with the data the points with error flags. There is qualitative agreement on the spectrum, but the theory somewhat exaggerates the beam-velocity peak, possibly indicating a greater weight on more central collisions than our model assumed. It is only fair to show the shortcomings of the theory, and in Fig. 14 the corresponding comparison for pi^+ are given. The theory vastly overestimates the Coulomb exclusion of beam-velocity pi^+. We believe this failure to be due to the classical nature of our calculation with neglect of quantum mechanical tunneling.

4. Summary

We have reviewed experiments on pion production in the velocity region of target or projectile. Our stopped-pion studies can only be regarded as exploratory, since we were not able to study a sufficient number of events. However, the results seem consistent with expectations from our pion inclusive studies near beam velocity. A sample of results from the 0^{o} spectrometer was presented. We then discussed two theoretical studies we had made that bear on the Coulomb effects on beam-velocity pions. We would encourage both emulsion experimentalists and theorists to address these problems for the further insights they may hold for high-energy, heavy-ion nuclear physics.

5. Acknowledgements

This work was supported mainly by the Office of Energy Research, Division of Nuclear Physics of the Office of High Energy and Nuclear Physics of the U.S. Department of Energy under Contract DE-AC03-76SF00098. Part support came from the Research Committee of the University of California, Berkeley. The support of Kuwait University for the sabbatical year at Berkeley of one of us (H.M.A.R.) is gratefully acknowledged.

REFERENCES

1. J. Chiba et al., Phys. Rev. C 20, 1332 (1979).
2. K. Nakai et al., Phys. Rev. C 20, 2210 (1979).
3. W. Benenson et al., Phys. Rev. Lett. 43, 683 (1979); errata, 44, 54 (1980).
4. J. P. Sullivan et al., Phys. Rev. C 25, 1499 (1982).
5. K. A. Frankel et al., Phys. Rev. C 25, 1102 (1982).
6. J. O. Rasmussen, Lawrence Lab Report LBL-14174 to be published in Proceedings of the Relativistic Heavy Ion Winter School, Banff, Alberta, Canada (Feb., 1982).
7. D. E. Greiner et al., Phys. Rev. Lett. 35, 152 (1975).
8. P. J. Lindstrom et al., Lawrence Berkeley Lab Report LBL 3650 (1975) unpublished.
9. E. M. Friedlander, Phys. Lett 2, 38 (1962).
10. N. I. Kostanashvili et al., Sov. J. Nucl. Phys. 6, 385 (1968).
11. N. I. Kostanashvili et al., Sov. J. Nucl. Phys. 13, 715 (1971).
12. N. I. Kostanashvili et al.. Sov. J. Nucl. Phys. 16, 542 (1973)
13. C. F. Powell, P. H. Fowler and D. H. Perkins, The Study of Elementry Particles by the Photographic Method, Pergamon Press, New York (1959).
14. S. Y. Fung et al., Phys. Rev. Lett. 40, 292 (1978).
15. G. Bertsch, Nature 283, 280 (1980).
16. K. G. Libbrecht and S. E. Koonin, Phys. Rev. Lett. 43, 1581 (1979).
17. J. Cugnon and S. E. Koonin, Nucl. Phys. A355, 477 (1981).
18. M. Gyulassy and S. K. Kauffmann, Nucl. Phys. A362, 503 (1981).
19. M. Bawin and J. Cugnon, Phys. Rev. C25, 387 (1982).

20. H. M. A. Radi, J. O. Rasmussen, K. A. Frankel, J. P. Sullivan, and H. C. Song, LBL Report-13768, (1982), Phys. Rev. C (to be published).

21. H. M. A. Radi, J. O. Rasmussen, J. P. Sullivan, K. A. Frankel, and O. Hashimoto, Phys. Rev. C25, 1518 (1982).

22. K. Van Bibber et al., Phys. Rev. Lett. 43, 840 (1979).

FIGURE LEGENDS

Figure 1. Photomicrograph of a stopped π-event initiated by 1.8A GeV ^{40}Ar ion in emulsion. The argon ion enters from the left, and the pion wanders downward, forming a "star" at the end.

Figure 2. Kinetic energy distribution of stopped π- (above) and π^+ (below) from Fe ions on heavy (Ag or Br) atoms. (Each bar represents one pion). The middle graph is for comparison from work of Reference 12 for three projectiles: 660 MeV protons (●), 9 GeV protons (X), and 60 Gev negative pions (O).

Figure 3. Same as Figure 2 except emulsion target nuclei undetermined.

Figure 4. Stopped-π^+ angular distributions, comparing projected angle Θ with data of Reference 12. At the bottom are our distributions in polar angle α (using dip angle information). Distributions a) (left) are for $E_\pi < 11.6$ MeV and b) (right) for 10 MeV $< E_\pi <$ 21.7 MeV.

Figure 5. Same as Figure 4 except for π^-.

Figure 6. Plot of our pion energies vs. estimated target residual charge Z_{eff}. The associated polar angle α and the azimuthal quadrant are indicated in parentheses. See text for azimuthal correlation explanation.

Figure 7. Schematic plan of the Zero-degree Pion Spectrometer JANUS.

Figure 8. Photograph looking upstream at JANUS spectrometer, in front are a few members of the research team, from L to R. Roy Bossingham, John Sullivan, Eunice Yoo, and Kenneth Frankel.

Figure 9. Isometric and contour plots of π^+ production cross sections for ^{20}Ne + NaF at 138A MeV. The Lorentz-invariant cross section is in units of b sr^{-1} GeV^{-2}.

Figure 10. Same as Figure 9 except at the higher energy of 655A MeV.

Figure 11. The π^- spectrum at 0° for Ne + C at 280A MeV. The three theoretical curves, corrected for experimental resolution, are for three values of the fragment velocity dispersion constant.

Figure 12. Scatter plot of Monte Carlo initial and final $\hat{v}_{\parallel}$ and $\hat{v}_{\perp}$ values for trajectories surviving absorption or capture into orbits. The plot is for one impact parmater 0.4 x grazing distance for the ^{20}Ne + ^{20}Ne system at 655A MeV.

Figure 13. Cut along 0° of impact-parameter-averaged π^- production cross sections. Data points are from experiment, and the histogram and smoothed line are from Monte Carlo theory.

Figure 14. Same as Figure 13 except for π^+

Figure 1

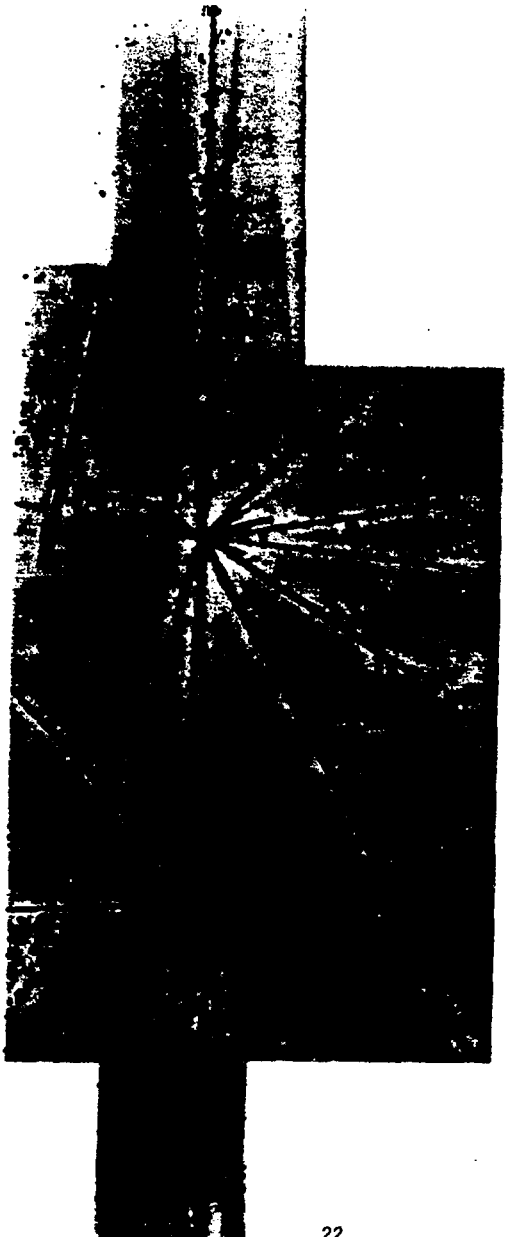

Fig. 2

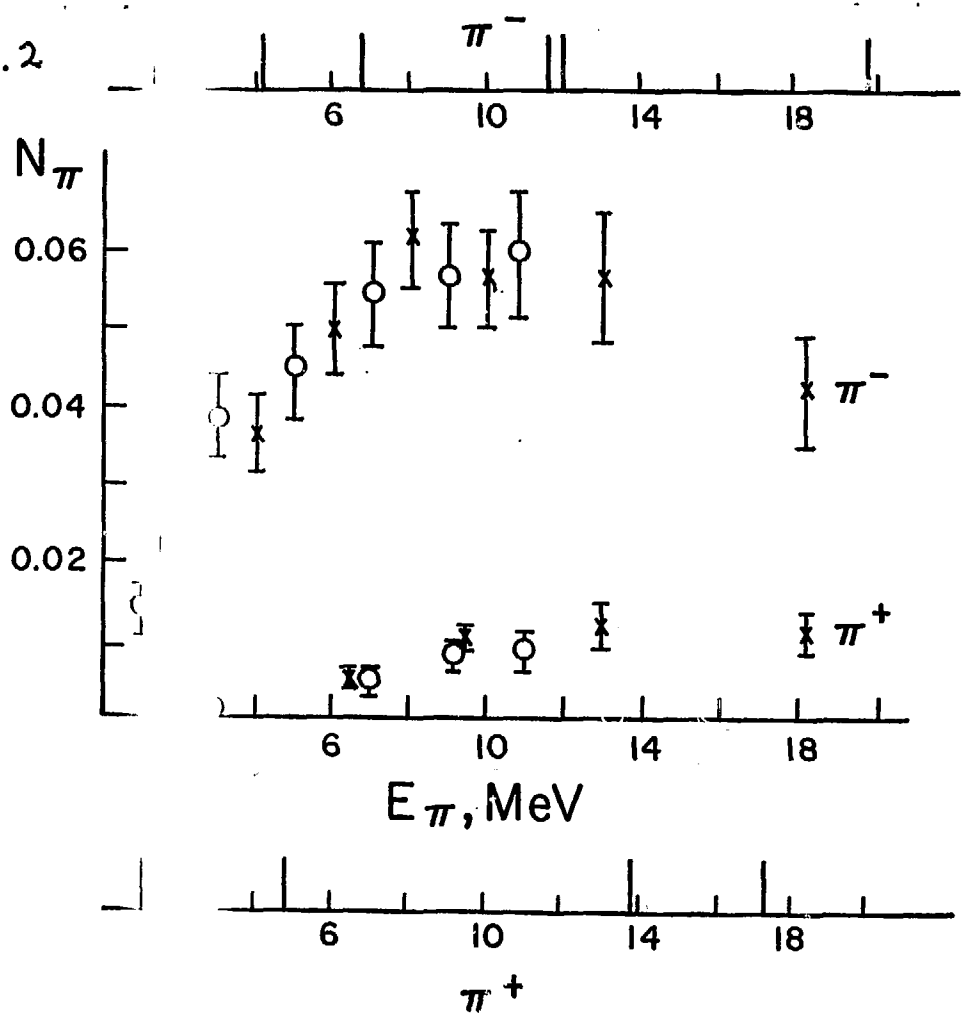

Fig. 3

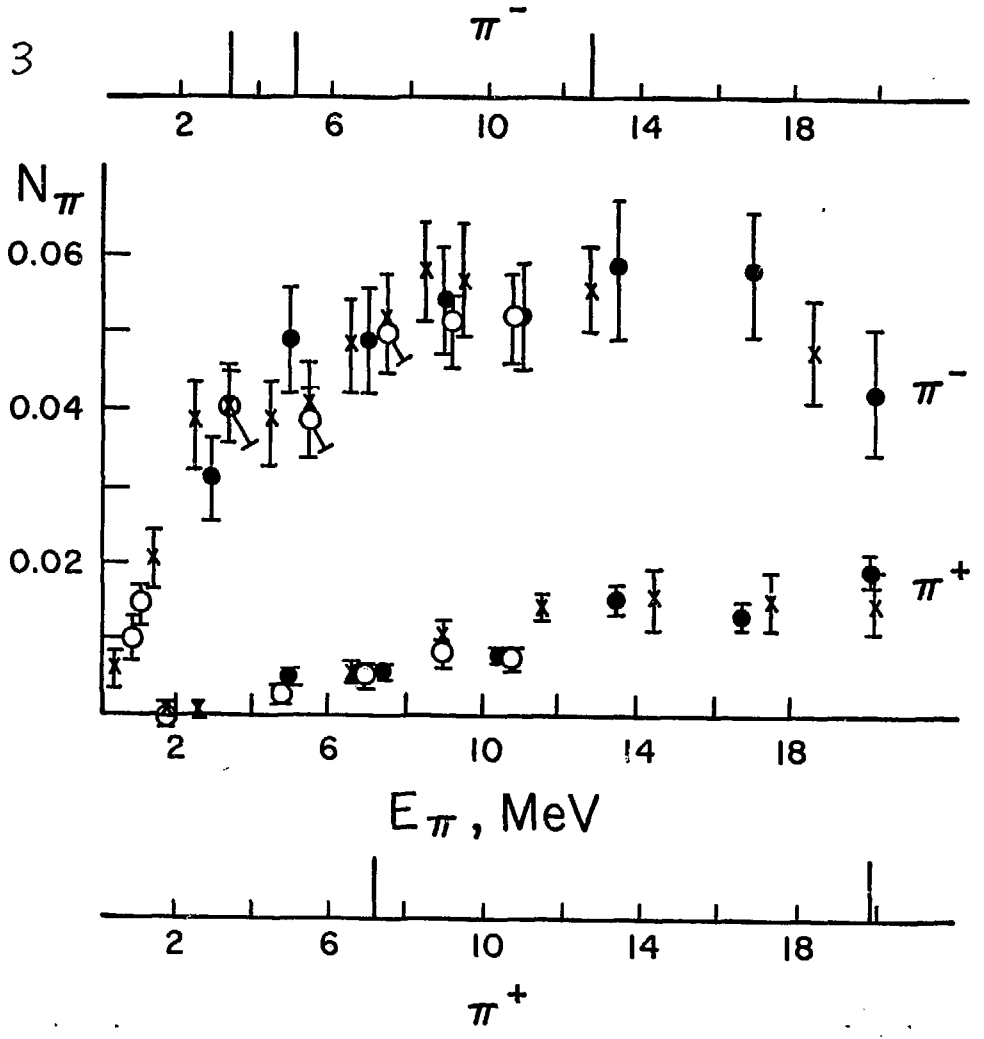

Fig. 4

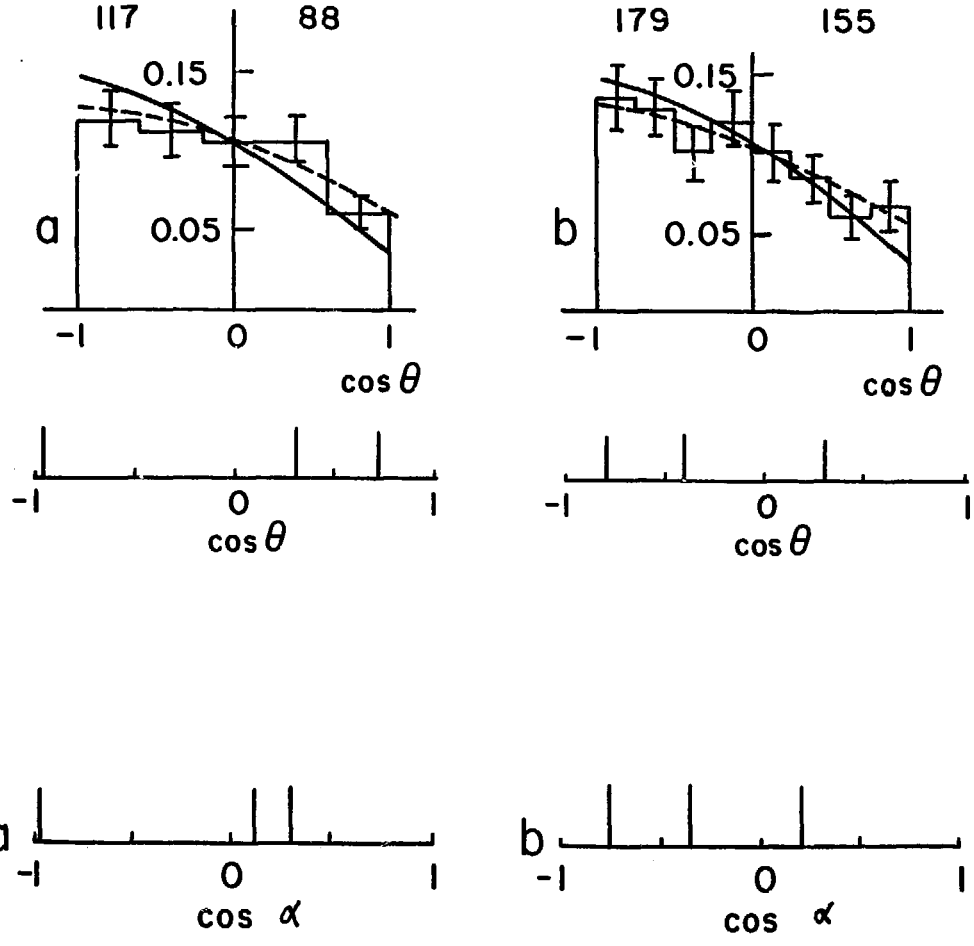
117
88
0.15
0.05
a
-1
0
1
cos θ
179
155
0.15
0.05
b
-1
0
1
cos θ
-1
0
1
cos θ
-1
0
1
cos θ
a
-1
0
1
cos α
b
-1
0
1
cos α

Fig. 5

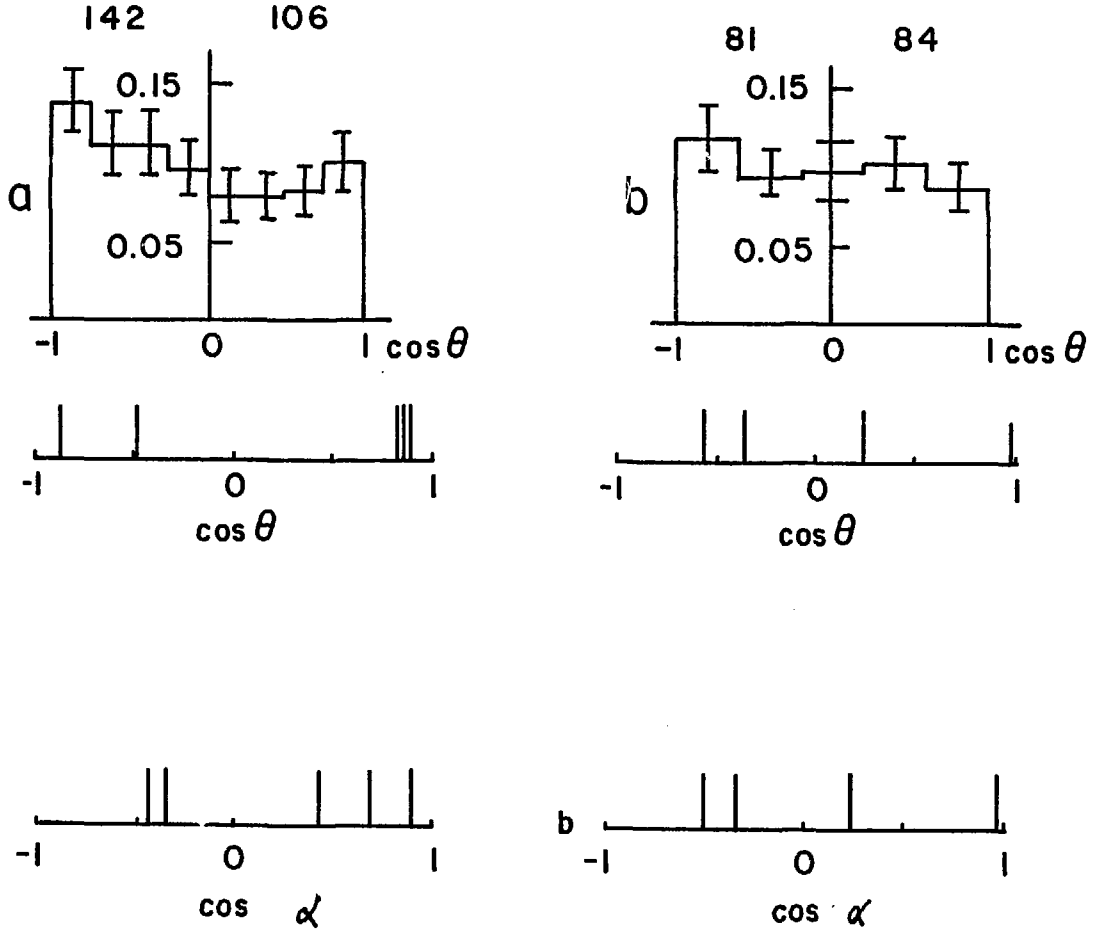
142
106
0.15
0.05
a
-1
0
1 cos θ
-1
0
1
cos θ
81
84
0.15
0.05
b
-1
0
1 cos θ
-1
0
1
cos θ
a
-1
0
1
cos α
b
-1
0
1
cos α

Fig. 6

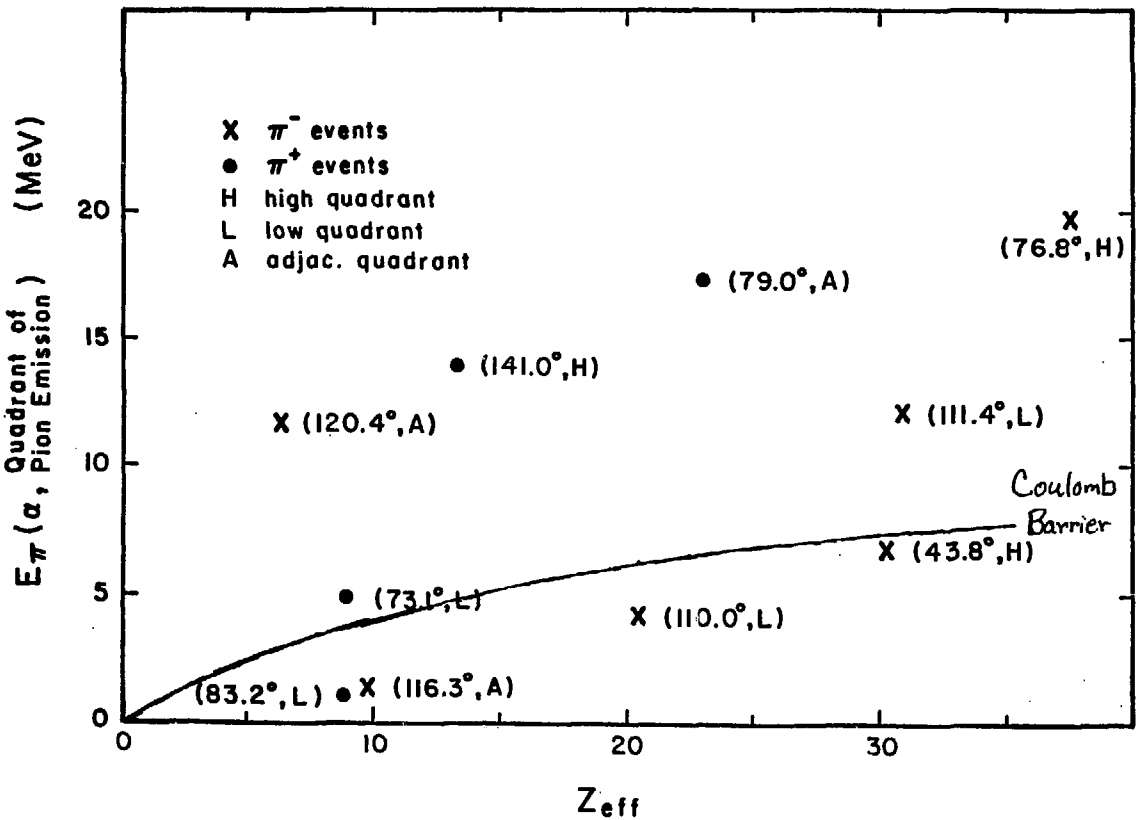
X π^- events
● π^+ events
H high quadrant
L low quadrant
A adjac. quadrant
X (76.8°,H)
● (79.0°,A)
● (141.0°,H)
X (120.4°,A)
X (111.4°,L)
Coulomb Barrier
X (43.8°,H)
● (73.1°,L)
X (110.0°,L)
(83.2°,L) ● X (116.3°,A)
E_π (α, Quadrant of Pion Emission) (MeV)
Z_{eff}
0
5
10
15
20
0
10
20
30

Fig. 7

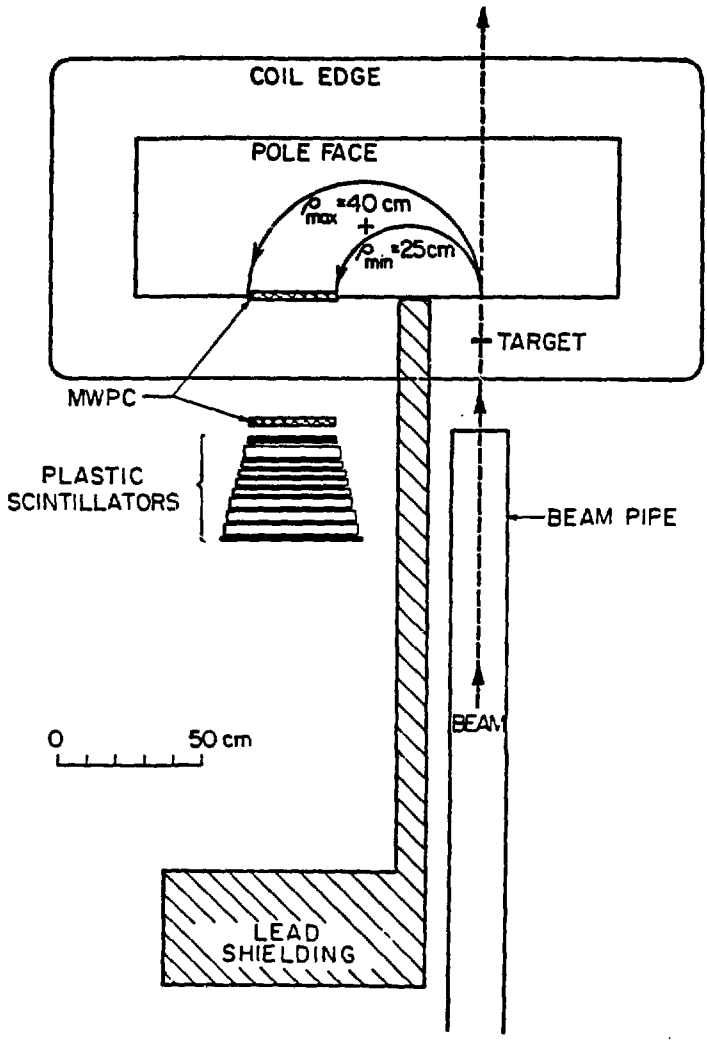

XBL7911-7291

Fig. 8 Mt. Selma Lab.

Fig. 9

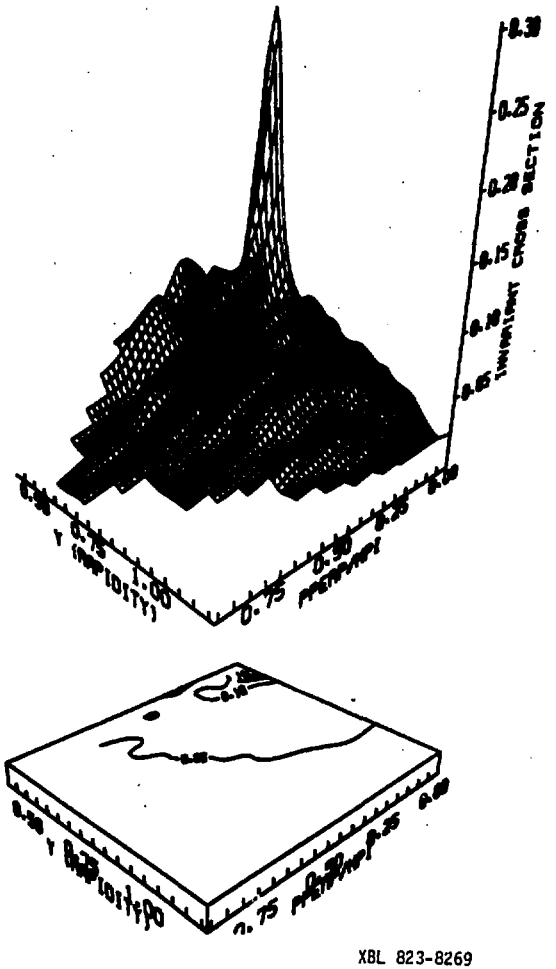

XBL 823-8269

Fig. 10

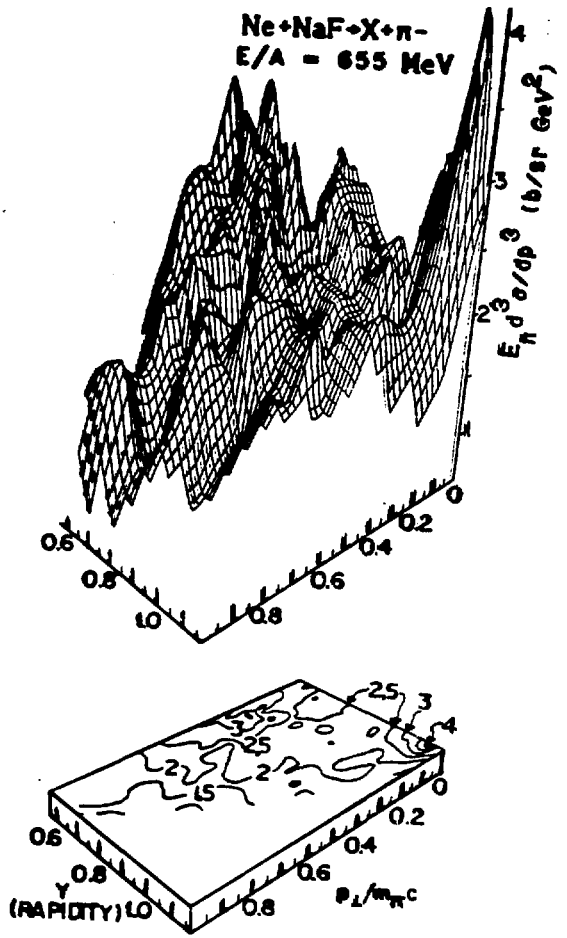
Ne+NaF→X+π-
E/A = 655 MeV
$E_\pi d^3\sigma/dp^3$ (b/sr GeV^2)
0
0.2
0.4
0.6
0.8
1.0
0.6
0.8
1.0
1
2
3
4
2.5
3
4
2.5
2
2
1.5
0
0.2
0.4
0.6
0.8
0.6
0.8
1.0
Y
(RAPIDITY)
$p_\perp/m_\pi c$

Fig.11

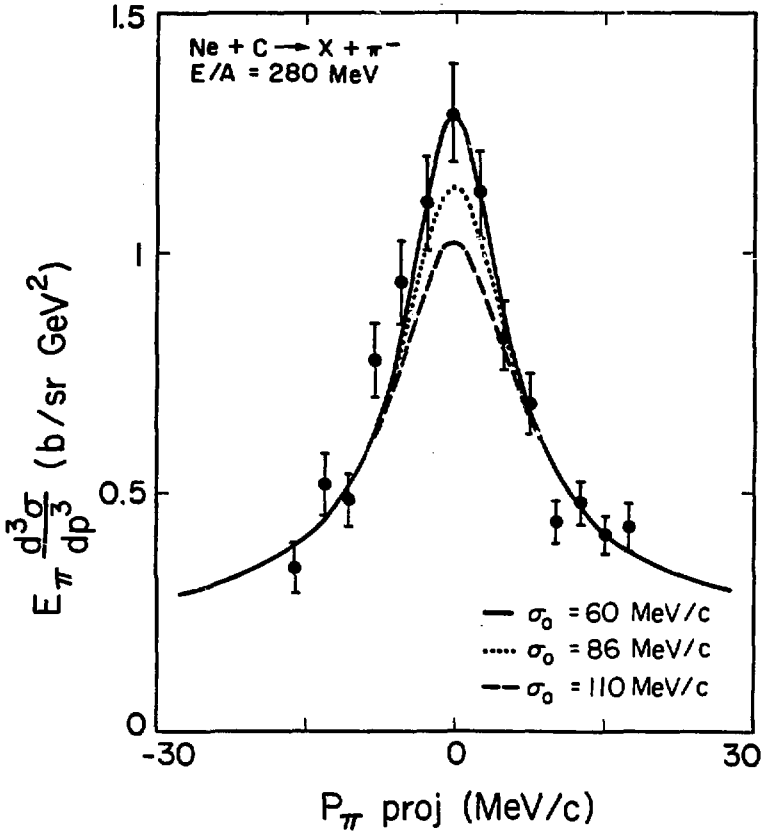
Ne + C → X + π⁻
E/A = 280 MeV
$E_\pi \frac{d^3\sigma}{dp^3}$ (b/sr GeV²)
P_π proj (MeV/c)
1.5
1
0.5
0
-30
0
30
σ₀ = 60 MeV/c
σ₀ = 86 MeV/c
σ₀ = 110 MeV/c

Fig. 12

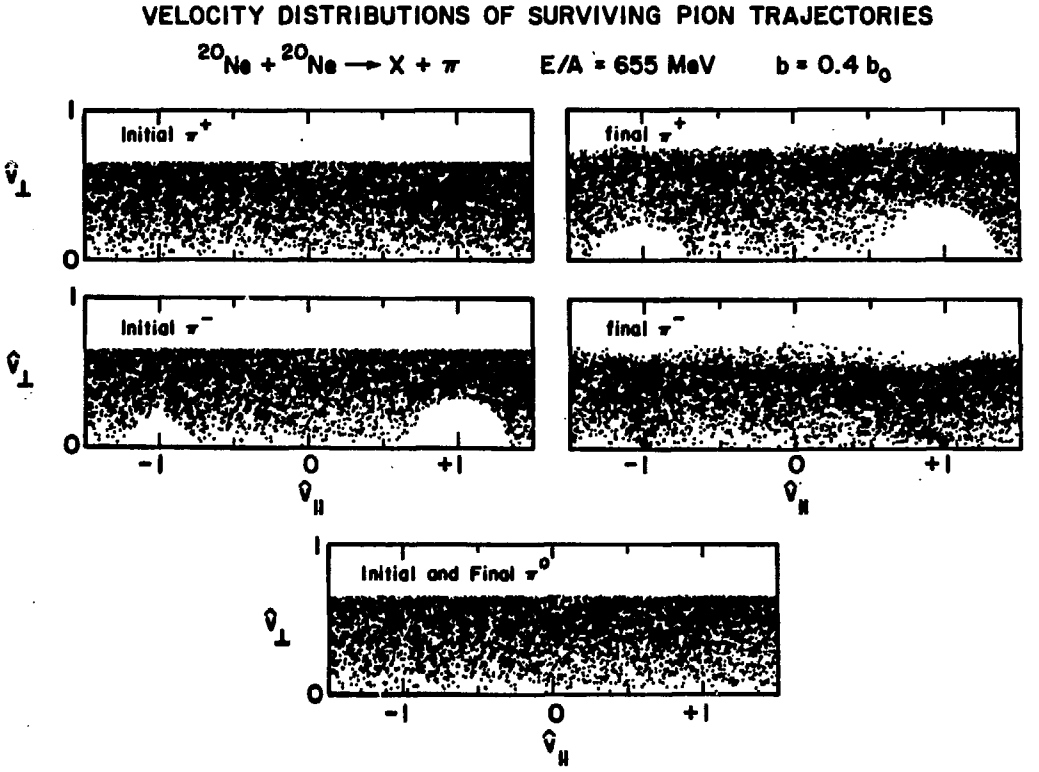
VELOCITY DISTRIBUTIONS OF SURVIVING PION TRAJECTORIES
$^{20}Ne + {}^{20}Ne \rightarrow X + \pi$ E/A = 655 MeV b = 0.4 b_0
Initial π^+
final π^+
Initial π^-
final π^-
Initial and Final π^0
$v_\perp$
$v_\parallel$
1
0
-1
+1

Fig. 13

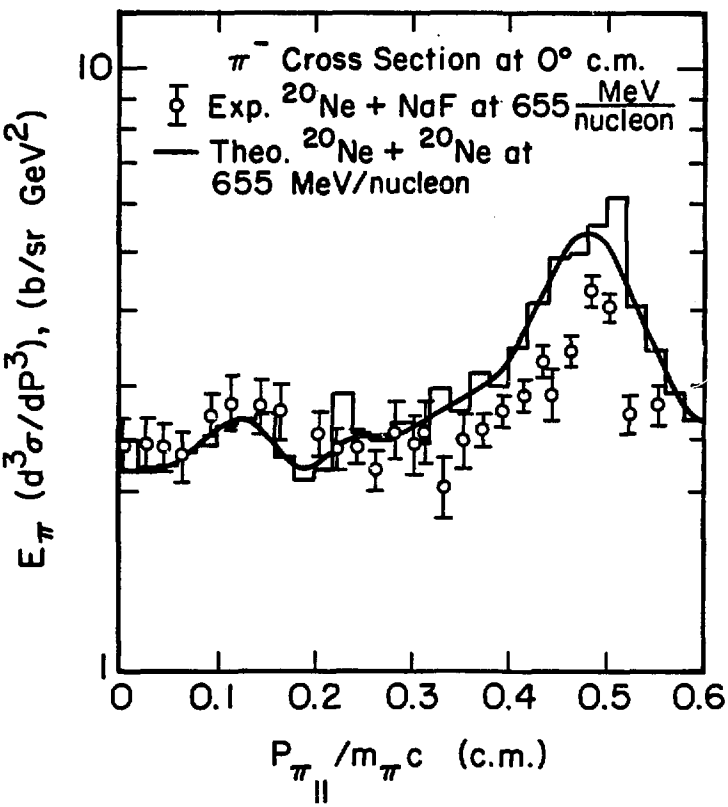
π^- Cross Section at 0° c.m.
Exp. ^{20}Ne + NaF at 655 $\frac{\text{MeV}}{\text{nucleon}}$
Theo. ^{20}Ne + ^{20}Ne at 655 MeV/nucleon
E_π ($d^3\sigma/dP^3$), (b/sr GeV^2)
10
1
0
0.1
0.2
0.3
0.4
0.5
0.6
$P_{\pi_{||}}/m_\pi c$ (c.m.)

Fig. 14

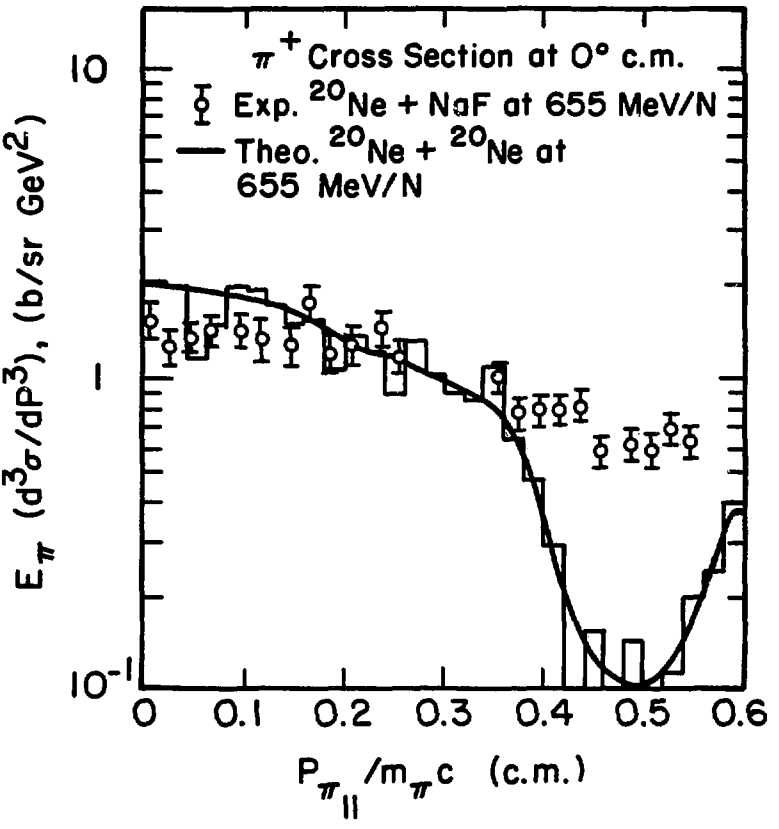
π^+ Cross Section at 0° c.m.
Exp. ^{20}Ne + NaF at 655 MeV/N
Theo. ^{20}Ne + ^{20}Ne at 655 MeV/N
E_π ($d^3\sigma/dP^3$), (b/sr GeV^2)
10
1
10^{-1}
0
0.1
0.2
0.3
0.4
0.5
0.6
$P_{\pi_{||}}/m_\pi c$ (c.m.)